Journal of Advances in Manufacturing Engineering
Web page info: https://jame.yildiz.edu.tr
DOI: 10.14744/ytu.jame.2024.00006

Original Article

Effect of strain rate on the tensile properties of 3D – printed PLA specimens with fused deposition modelling

Sara Saeed Abdulrahman ELTAHİR[1], Roaa GOMAA[2], Çağatay YILMAZ[*2]

[1]*Department of Advanced Materials and Nanotechnology, Abdullah Gül University, Kayseri, Türkiye*
[2]*Department of Mechanical Engineering, Abdullah Gül University, Kayseri, Türkiye*

ARTICLE INFO

Article history
Received: 11 July 2024
Revised: 22 August 2024
Accepted: 11 September 2024

Key words:
Strain rate, fused deposition modeling (FDM), polylactic acid (PLA), digital image correlation (DIC), tensile testing.

ABSTRACT

Many engineering applications and industries require components to be lightweight while still maintaining strong mechanical properties. Polylactic acid (PLA) is widely used in additive manufacturing due to its biodegradability, ease of printing, and favourable mechanical characteristics, making it an in-demand material for various applications. Understanding the influence of strain rate on the tensile properties of PLA is crucial, as it directly affects the material's performance under different loading conditions. This research investigates the influence of strain rate on the tensile properties of PLA material fabricated through fused deposition modeling (FDM) using Type V ASTM D638 – 14 specimens. Three distinct strain rates (0.8 mm/min, 2 mm/min, and 20 mm/min) are considered, and Digital Image Correlation (DIC) is employed for ultimate tensile strain analysis. The methodology involves CAD modeling, 3D printing, surface preparation, and tensile testing, with DIC analysis performed using the Ncorr application. Results indicate a linear increase in tensile strength with higher strain rates as the tensile strength increased by 30% from 40.41 MPa at 0.8 mm/min to 52.62 MPa at 20 mm/min. Additionally, Elastic modulus increases with increasing strain rate, rising by approximately 43.5%, from 1.54 GPa at 0.8 mm/min to 2.21 GPa at 20 mm/min. This research contributes valuable insights into the dynamic behavior of FDM-printed PLA under different strain rates, offering implications for material performance in applications requiring diverse loading conditions.

Cite this article as: Eltahir, A. S. S., Gomaa, R., & Yılmaz, Ç. (2024). Effect of strain rate on the tensile properties of 3D – printed PLA specimens with fused deposition modelling. *J Adv Manuf Eng*, 5(2), 00–00.

INTRODUCTION

Additive manufacturing (AM), or 3D printing, stands out as a highly multifunctional and promising technology in advanced manufacturing. AM includes various processes, as discussed by Wong and Hernandez [1] such as stereolithography (SLA), fused deposition modelling (FDM), laminated object manufacturing (LOM), selective laser sintering (SLS), laminated engineered net shaping (LENS), and electron beam melting (EBM). Notably, FDM is recognized as one of the most extensively utilized methods for working with thermoplastic polymeric materials. Utilizing this technique involves the incremental deposition of layers.

FDM has distinguishable characteristics as, highlighted by Singh et al. [2], including its user-friendly interface, cost-effectiveness, and environmentally sustainable characteristics, which make it advantageous in the domains of prototyping and manufacturing. According to Kristiawan et al. [3], it was revealed that a predominant 51% of products manufactured using AM technology belong to the cat-

***Corresponding author.**
*E-mail address: yilmaz.cagatay@agu.edu.tr

egory of polymer-plastic filaments. This dominance can be attributed to the favorable characteristics of these materials, which not only meet essential criteria for utilization and advancement but also contribute significantly to enhancing the efficiency and manageability of FDM processes. Among the polymers employed in this technique, PLA stands out as a particularly noteworthy material for its widespread application and effectiveness in 3D printing applications.

Recent studies have explored the impact of strain rate on the mechanical properties of PLA 3D-printed materials. For example, Ali et al. [4] investigated the relationship between strain rate and mechanical properties of 3D-printed PLA materials using various input parameters like infill density, build orientation, layer height, and strain rate, finding that the strain rate has a moderate impact on the mechanical properties, contributing about 13.56% to the overall mechanical behaviour, with higher strain rate (10 mm/min) improving mechanical properties such as modulus, ultimate tensile and yield strength, toughness, and resilience. The Taguchi design suggested that an optimal strain rate of 5 mm/min, combined with 100% infill density and a 0.1 mm layer height, could yield better results, particularly in improving resilience by 21.83%. Similarly, Hodžić et al. [5] investigated the influence of strain rate on the tensile properties of various FDM materials, including PLA, across a range of strain rates - 0.5 mm/min to 100 mm/min. The findings reveal a linear rise in tensile and yield strength as strain rates escalate, underscoring the material's robustness under dynamic loading conditions. Additionally, Elastic modulus exhibits an ascending trend with elevated strain rates. As a noteworthy observation, a notable reduction in testing time with the increase in strain rates, such as PLA material testing time decreased up to 99.58%. Further, Vidakis et al.'s [6] investigated the strain rate sensitivity of five thermoplastic polymers, including PLA, using ASTM D638 – 14 for specific Type V specimens. The study explores the tensile properties of test specimens subjected to varying strain rates (10, 25, 50, 75, and 100 mm/min). They observed similar increase in tensile strength, yield strength, and modulus with rising strain rates. The brittleness of PLA became more pronounced at higher strain rates, particularly at 50 mm/min. As a noteworthy observation, PLA's elevated strain rate sensitivity, suggesting the necessity for further exploration and potential enhancements.

In related research, studies have explored the influence of strain rate on the mechanical properties of different filament materials used in 3D-printing, such as Ergene and Bolat [7] studied the effect of strain rate on the mechanical properties of FDM 3D printed polyethylene terephthalate glycol (PETG) specimens, showing that while lower strain rates generally yield higher tensile strength and more ductile deformation, higher strain rates enhanced tensile strength for thicker layers but resulted in more brittle failure modes. Specifically, specimens with a 0.1 mm layer thickness exhibited peak tensile strength at lower strain rates, whereas thicker layers (0.2 mm and 0.4 mm) showed greater tensile strength at higher strain rates. Additionally, as strain rates increase, the deformation mechanism shifts from ductile to brittle. Furthermore, Wang et al. [8] studied the influence of infill parameters and tensile strain rate on the overall mechanical characteristics of polyamide-based composites reinforced with short carbon fibers (Onyx®) produced using FDM. The study involved strain rates— 2.78×10^{-4} mm/min, 2.78×10^{-5} mm/min, and 2.78×10^{-6} mm/min. They reported enhanced tensile strength and elastic modulus at higher strain rates, though elongation decreased. Additionally, there was an observed increase in the relative energy absorption capacity with higher tensile strain rates. Hence, there is a strong correlation between higher rates and enhanced mechanical properties. Along similar lines, Wang et al. [9] studied the material polyurethane acrylate resin produced by Digital Light Processing (DLP) 3D printing, demonstrated that higher strain rates - 0.06 mm/min and 0.6 mm/min- improved the ultimate tensile strength and elastic modulus in both tension and compression testing.

Hence, these studies collectively investigated various AM 3D printing techniques and diverse polymer-plastic filaments, it becomes apparent that an intricate interplay exists between strain rate and mechanical characteristics within the realm of FDM 3D printed materials. The anticipated outcomes of escalating the strain rate include an increase in Ultimate Tensile Strength, Yield Tensile Strength, and Elastic Modulus. This study will investigate the influence of strain rate on the tensile properties of PLA material, with a particular focus on exploring strain rate values that have not been examined in the existing literature. Table 1 provides a comprehensive summary of the strain rate ranges investigated in existing literature.

Upon examining the existing literature regarding FDM and PLA, it becomes apparent that considerable attention has been directed towards exploring the impact of 3D printing parameters on the mechanical characteristics of printed parts. In addition, the assessment of mechanical properties in these studies primarily relies on conducting mechanical tests, such as tensile testing, on samples produced with varying 3D printing parameters. This observation is supported by the findings of a study conducted by Hosseini et al.[19], highlighting that previous research has predominantly centered on examining the influence of 3D printing parameters on the mechanical characteristics of printed materials. While a few researchers have explored strain rate effects in polymer blends manufactured through conventional methods like injection molding with polycarbonate, scarce attention has been given to investigating the strain rate sensitivity of PLA polymers produced using FDM.

Consequently, the main objective of this study is to investigate the influence of strain rate on the tensile properties of PLA material using Type V ASTM D638 – 14 specimen types. Three distinct strain rates, 0.8 mm/min, 2 mm/min, and 20 mm/min, corresponding to 0.0133 mm/s, 0.0333 mm/s, and 0.333 mm/s, respectively, were utilized. Both 0.8 mm/min and 2 mm/min fall within the medium strain rate range, whereas 20 mm/min is classified as a high strain rate. A tensile test was performed and analyzed using the Digital Image Correlation (DIC) method.

Table 1. Overview of strain rates in additively manufactured (3D printed) models from literature

Filament material	Printing method	Strain rate values	Article reference
PLA, tough PLA, and carbon PLA	3D-FDM printing	0.5, 1, 5, 50, and 100 mm/min	[5]
PLA, ABS, PETG, PA6, and PP	3D-FDM printing	10, 25, 50, 75, and 100 mm/min	[6]
Polyamide-based composites (Onyx®) reinforced with short carbon fibers	3D-FDM printing	The corresponding strain rates were 2.78×10^{-4}, 2.78×10^{-5} and 78×10^{-6} mm/min	[8]
PUA	DLP printing	0.001 s^{-1} and 0.01 s^{-1}	[9]
ABS	3D-FDM printing	1.27, 5, 50 and 100 mm/min	[10]
ABS	3D-FDM printing	Constant at 6 mm/min	[11]
PLA and TPU	3D-FDM printing	0.45, 0.30, 0.123, 6.104 and 3.428 mm/min	[12]
PMMA	TPL technique	6 orders of magnitude of strain rate, from $7e^{-4}$ to 600 s^{-1}	[13]
Nylon reinforced by short carbon fiber (Onyx)	FFF printing	1, 10, 50 and 100 mm/min	[14]
CRFRC	3D-FDM printing	33360, 80100, 145920 and 185820 mm/min	[15]
Graphene/grey resin - PMMA nanocomposites	3D-FDM printing	High strain rate (~1000/s) Low strain rate (~1/s)	[16]
PEEK/HAP-rGO composites	3D-FDM printing	Low strain rates 0.001, 0.01, and 0.1 s^{-1} High strain rates of 800 s-1 and 1000 s^{-1}	[17]
3D-printed composites: Nylon white and Onyx	3D- FFF printing	Nylon: 5, 50, 300 mm/min Onyx: 1.3, 127.5, 255 mm/min	[18]
CPE+ and nylon. PLA, ABS, and PC	3D-FDM printing	2.5, 13, 50, 200 and 400 mm/min	[19]
Polyamide-based composite	3D-FDM printing	Low strain rates: 8×10^{-4} s^{-1}, and 8×10^{-3} s^{-1} High strain rate: 1700 s^{-1} and 3510 s^{-1}	[20]
CNT-PLA composites	3D-FDM printing	Constant at 1 mm/min	[21]
TS polymers	Delta-type 3D printer	The shear strain rate varies from ~4 to ~100 s^{-1}	[22]

PLA: Polylactic acid; FDM: Fused deposition modelling; 3D: 3-Dimentional; PLA: Polylactic acid; ABS: Acrylonitrile butadiene styrene; PETG: Polyethylene terephthalate glycol; PA6: Polyamide 6; PP: Polypropylene; PUA: Polyurethane acrylate; DLP: Digital light processing; TPU: Thermoplastic polyurethane; PMMA: Polymethylmethacrylate; TPL: Twophoton lithography; FFF: Fused filament fabrication; CRFRC: Continuous ramie fiber reinforced biocomposites; PEEK: Polyetheretherketone; HAP: Hydroxyapatite; rGO: Reduced graphene oxide; CPE: Chlorinated polyethylene; CNT: Carbon nanotubes; TS: Thermoplastic sulfones.

MATERIALS AND METHODS

PLA specimens were produced using Fused Deposition Modeling. The initial phase involves the development of CAD models corresponding to the standardized dimensions outlined by ASTM D638 – 14 for Type V. Following this, the specimens were 3D printed, and preparatory steps, including surface preparation, were taken before conducting the tensile test. To analyze the test outcomes, the Digital Image Correlation (DIC) method is applied, utilizing the open-platform Ncorr application. The data obtained from Ncorr undergoes further processing and refinement using MATLAB – (R2022b MATLAB 9.13) – to compute the tensile properties for all specimens.

Specimen Design Model

The selection of Type V specimen was decided by considering the required printing time and filament usage of the specimen when compared to Type I-IV. As displayed in Table 2, it is found that Type V is the most cost-efficient ASTM-D638 type. Type V specimen dimensions followed the guidelines outlined in the ASTM- D638 – 14 standards, as illustrated in Table 3 and Figure 1. Utilizing SOLIDWORKS software – (SOLIDWORKS® - 2022), 3D models of the specified specimen type were created. The 3D model was converted to Stereolithography (.STL) file format, ensuring compatibility with the Raise 3D – (Raise3D N2 Plus) – printer.

Table 2. Cost effectiveness of the 5 types of ASTM-D638 standard

Sample type	Printing time	Filament usage
Type I	1 hour, 18 minutes, 31 seconds	9.8 grams/3.30 meter
Type II	1 hour, 9 minutes, 45 seconds	8.3 grams/2.80 meter
Type III	3 hour, 5 minutes, 27 seconds	23 grams/7.70 meter
Type IV	48 minutes, 38 seconds	5.7 grams/1.91 meter
Type V	14 minutes, 59 seconds	1.8 grams/0.60 meter

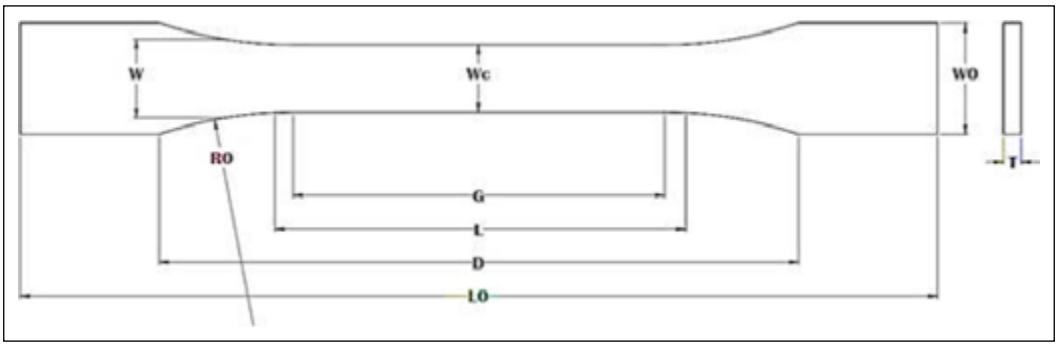

Figure 1. ASTM D638 – 14 type V test specimen.

Table 3. ASTM- D638 – 14 Type V dimensions [23]

Labels	Dimension (mm)	Tolerance (mm)
W-width of narrow section	3.18	±0.5
L-length of narrow section	9.53	±0.5
WO-width overall	9.53	+3.18
LO-length overall	63.5	–
G-gage length	7.62	±0.25
D-distance between grips	25.4	±5
R-radius of fillet	12.7	±1
Thickness	3.2	±1

Table 4. Printing parameters

3D printing parameter	Values
Filament type	PLA
Layer thickness (mm)	0.25
Infill density (%)	100
Infill angle	0
Filling structures	Solid lines
Filament extruder temperature (°C)	215
Heatbed temperature (°C)	80
Extruder nozzle	1
Extruder width (mm)	0.38
First layer speed (mm/s)	8
Speed (mm/s)	30
Retraction speed (mm/s)	20
Shell numbers	1
Processor	IdeaMaker – (version 4.4.0 Alpha)
Platform addition – brim numbers	10

PLA: Polylactic acid.

Table 5. PLA material specifications [25]

Filament properties	Values
Filament type	PLA
Brand	eSun
Model	PLA+
Weight (Kg)	1 Kg/spool
Color	Red
Filament diameter (mm)	1.75±0.05
Filament length (m)	340–345
Printing temperature (°C)	210–230
Density (g/cm^3)	1.23
Tensile strength (MPa)	60
Bending strength (MPa)	74
Flexural modulus (MPa)	1973
IZOD impact strength (kJ/m^2)	6

PLA: Polylactic acid.

3D: Printing

The choice of printing parameters was done as following the previous study of our lab [24] and outlined in Table 4.

In this study, 18 PLA specimens were 3D printed with the PLA material specifications demonstrated in Table 5, with six specimens designated for each strain rate value. A quality control process was implemented by using a calliper, thoroughly examining the dimensions of the specimens to ensure compliance with the established ASTM- D638 – 14 standards. Successful printing was characterized by the absence or minimal presence of defects and a seamlessly smooth surface on the specimen. It is noteworthy that all printed specimens met these criteria. Table 6 presents the dimensional measurements for the printed specimens, specifically their width and thickness. The data indicate that the specimens consistently maintained an average width of 3.2 mm and an average thickness of 3.4 mm, with minimal variation across all samples. These results align with the findings of Bolat and Ergene [26], who examined the dimensional accuracy and surface quality of 3D printed tensile test samples made from PLA, PET-G, and ABS. They reported that PLA samples achieved the highest width accuracy, with an average accuracy level exceeding 97.7%, and exhibited the best surface quality (2.65 μm) due to PLA's excellent bonding capacity.

For DIC analysis during tensile tests, specimens were prepared by coating their surfaces with opaque white spray paint. The coating, typically 2-3 layers, was applied until uniform coverage. To fulfil DIC parameter needs, a black speckle pattern was manually added onto the white-coated

Table 6. Printed specimens measurements

No.	Width (mm)			Avg	Thickness (mm)			Avg
1	3.2	3.2	3.2	3.2	3.4	3.4	3.4	3.4
2	3.2	3.2	3.2	3.2	3.4	3.4	3.4	3.4
3	3.2	3.2	3.2	3.2	3.4	3.4	3.4	3.4
4	3.2	3.2	3.2	3.2	3.4	3.4	3.4	3.4
5	3.2	3.2	3.2	3.2	3.4	3.4	3.4	3.4
6	3.2	3.2	3.2	3.2	3.4	3.4	3.4	3.4
7	3.2	3.2	3.2	3.2	3.4	3.4	3.4	3.4
8	3.2	3.1	3.2	3.17	3.4	3.4	3.4	3.4
9	3.2	3.2	3.2	3.2	3.4	3.4	3.4	3.4
10	3.2	3.2	3.2	3.2	3.4	3.4	3.4	3.4
11	3.2	3.2	3.2	3.2	3.4	3.4	3.4	3.4
12	3.2	3.2	3.2	3.2	3.4	3.5	3.4	3.43
13	3.2	3.3	3.2	3.23	3.4	3.4	3.4	3.4
14	3.2	3.2	3.2	3.2	3.4	3.4	3.4	3.4
15	3.2	3.2	3.2	3.2	3.4	3.4	3.4	3.4
16	3.2	3.2	3.2	3.2	3.4	3.4	3.4	3.4
17	3.2	3.2	3.2	3.2	3.4	3.4	3.4	3.4
18	3.2	3.2	3.2	3.2	3.4	3.4	3.4	3.4
Avg				3.2				3.4

Figure 2. Surface spackle pattern preparation of tested 18 specimens.

surface, ensuring thorough coverage across all specimens. A soft-bristled toothbrush was utilized to create the speckle pattern. An example of this is shown in Figure 2.

Tensile Testing

Tensile tests were conducted on printed specimens using a Shimadzu testing machine. The machine operated at constant settings to avoid the influence of other testing parameters. Only the impact of strain rate on part behaviours and mechanical properties was studied. Strain rates of 0.8 mm/min, 2 mm/min, and 20 mm/min were employed. Each strain rate value was tested with six identical tensile specimens, and the results were represented by taking the mean values. The gauge length was precisely set according to ASTM D638 – 14 standards.

For the Digital Image Correlation (DIC) system, a high-resolution cell phone camera with a 26 mm focal length, f/1.8 lens, 50-megapixel resolution, and 1080 pixels at 30 frames per second was mounted on a stable tripod at an optimal distance from the specimen. Careful consideration was given to ensure recording quality, with two tripods holding flashlights at the same distance as the camera to provide sufficient brightness. The recording duration was precisely synchronized with the tensile testing machine's operation, capturing the entire process from initiation to fracture occurrence.

Ncorr Analysis

Utilizing the open-platform Ncorr application, the DIC method was used to analyze recorded specimen data. Initially, the videos were converted into a series of images at 30 frames per second. For 0.8 mm/min, 61 to 340 images were analyzed, 2 mm/min had 25 to 138 images, and 20 mm/min had the fewest images, ranging from 10 to 19.

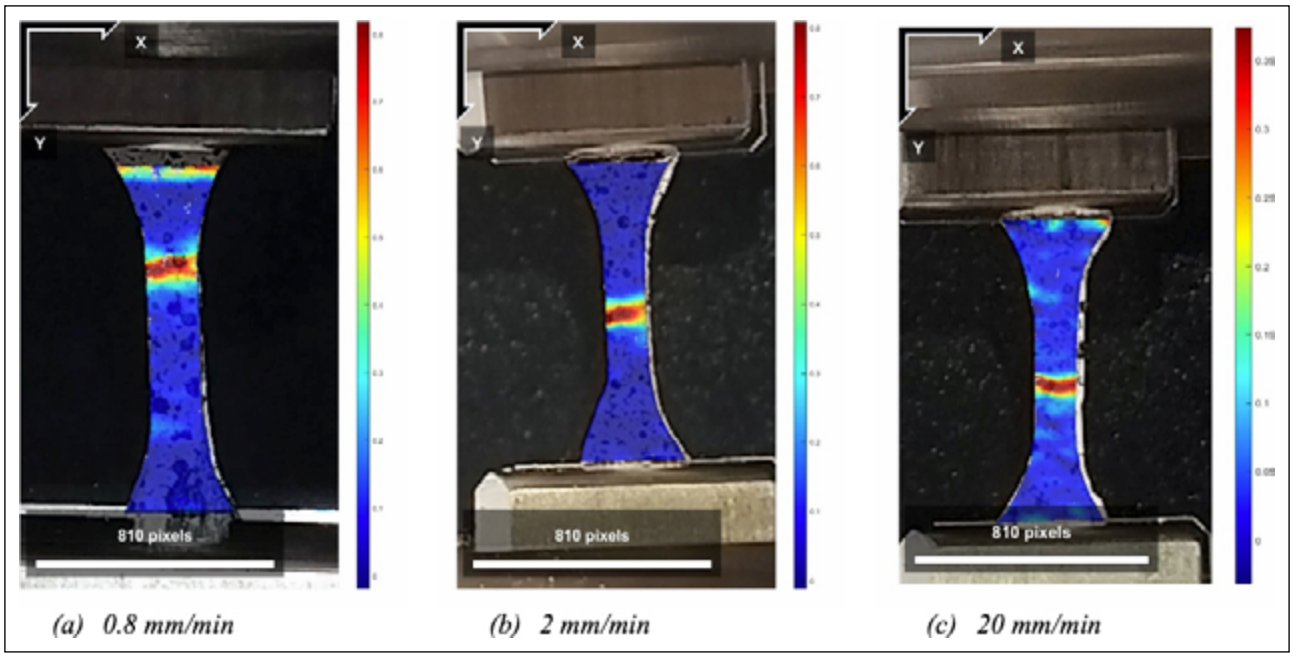

Figure 3. Strain field obtained from Ncorr analysis **(a)** E_{yy} for strain rate of 0.8 mm/min **(b)** E_{yy} for strain rate of 2 mm/min **(c)** E_{yy} for strain rate of 20 mm/min.

Table 7. DIC parameters

DIC data	
Phone frame rate	30 fps
Video conversion rate	1 image/sec
Ncorr parameters	
Subset radius	33
Subsets spacing	1
Num thread	1
Seeds number	1

DIC: Digital image correlation.

MATLAB facilitated the DIC analysis of these images. The Ncorr program was executed with the command "handles_ncorr = ncorr," enabling file compilation and accessing the program menu for image and DIC parameter arrangement. The analysis started with the selection of a reference image, representing the initial state. Subsequent images were then compared to the reference for deformation analysis within a defined region of interest (ROI). The DIC computation process includes adjusting several parameters like subset radius, subset spacing, number of threads, and seeds. A subset radius of 33 units, minimizing noisy strain data, a subset spacing of 1 unit, and both thread and seed numbers of 1 were chosen based on prior project results as well the requirements for the small size of Type V specimens, shown in Table 7. After analyzing displacement, the strain values were calibrated and scaled by converting pixel values to millimeters for measurable displacement. The computed strain values for E_{xx}, E_{xy}, and E_{yy} planes were saved in a MATLAB Data (.mat) file for additional analysis and processing. E_{xx} is lateral strain, E_{yy} is longitudinal strain, and E_{xy} is in-plane shear strain.

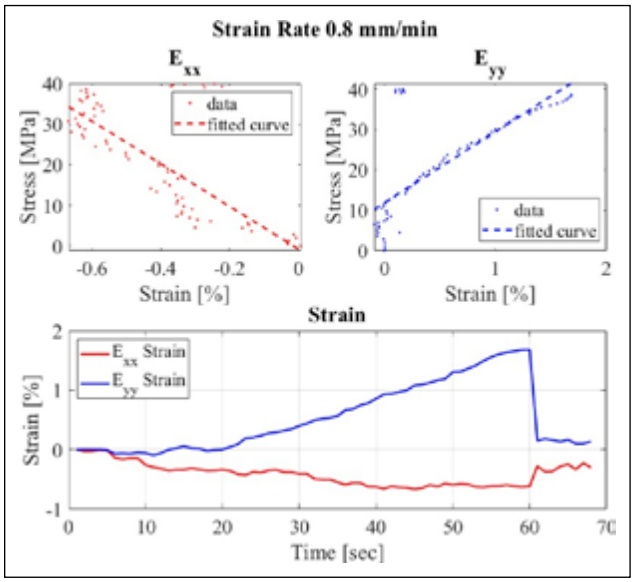

Figure 4. Strain rate 0.8 mm/min Ncorr results **(a)** E_{xx} stress-strain curve **(b)** E_{yy} stress-strain curve **(c)** Average strain for E_{xx} and E_{yy}.

Post Data Analysis

Processed through MATLAB, the Ncorr displacement analysis data, which includes information from the tensile machine and Ncorr, was imported. The tensile machine data, including force and stroke measurements over time, were used in stress calculation by dividing force by the specimen's cross-sectional area. The maximum stress for each tested specimen corresponding to strain rate values - 0.8 mm/min, 2 mm/min, and 20 mm/min- was extracted to calculate the average Ultimate Tensile Strength for each strain rate value. For the Ncorr displacement data analysis,

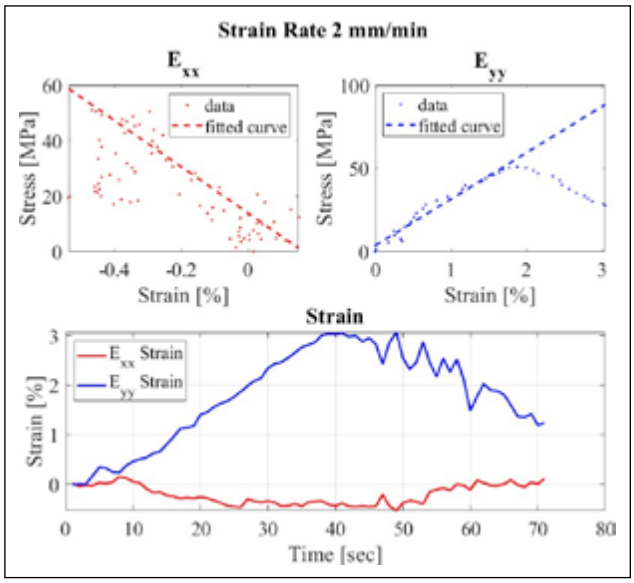

Figure 5. Strain rate 2 mm/min Ncorr results **(a)** E_{xx} stress-strain curve **(b)** E_{yy} stress-strain curve **(c)** Average strain for E_{xx} and E_{yy}.

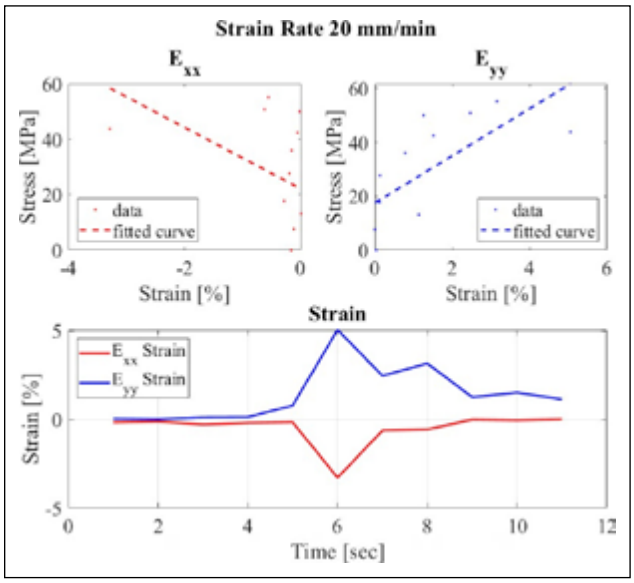

Figure 6. Strain rate 20 mm/min Ncorr results **(a)** E_{xx} stress-strain curve **(b)** E_{yy} stress-strain curve **(c)** Strain for E_{xx} and E_{yy}.

strain values are refined by filtering out non-zero values in each frame and eliminating irrelevant zero values. Average strain (E_{xx} and E_{yy}) for each frame is computed using the refined data. To align with the stress data, which has significantly more data points, the strain values were interpolated, facilitating the presentation of the stress-strain curve on the same graph.

RESULTS AND DISCUSSION

Ncorr analysis of the DIC provided comprehensive strain and displacement data from the tensile test, including a 2D strain field (as shown in Fig. 3). Following post-data analysis, a set of three graphs were generated by the MATLAB code; the stress-strain curve of E_{xx}, the stress-strain curve of E_{yy}, and the average strain curve of E_{xx} and E_{yy} with respect to the time. Given that the study involved 18 specimens subjected to three different strain rates, various similar chart outcomes were obtained from each test. Consequently, this report focuses on discussing chart results from one specimen for each type to avoid redundancy.

The results of Ncorr for a strain rate of 0.8 mm/min are illustrated in Figure 4. The graph clearly shows a decreasing trend in the E_{xx} stress-strain curve, suggesting a reduction in specimen width under tensile force. In contrast, the E_{yy} stress-strain curve shows an upward trend, indicating elongation as tensile force is applied. The average strain values for E_{xx} and E_{yy} are also provided. Notably, the E_{yy} strain demonstrates an increasing slope until the point of fracture, while the E_{xx} strain decreases.

The results of Ncorr for a strain rate of 2 mm/min are illustrated in Figure 5. Similar to the previous results, the E_{xx} stress-strain curve decreases while the E_{yy} stress-strain curve increases with strain. However, there are noticeable inconsistencies in the data points of the stress-strain curves, presenting a scattered and noisy pattern. Likewise, the average values of E_{xx} and E_{yy} exhibit spiky behavior. These irregularities may stem from difficulties encountered in accurately detecting speckle patterns during the Ncorr displacement analysis. Figure 6 shows the Ncorr results for a strain rate of 20 mm/min, and similar spiky behavior is observed. This tendency could be attributed to fewer frames available for analysis due to the higher strain rate, indicating that faster displacements occur for the DIC analysis to detect.

In Figure 7a, an evident linear increase in tensile strength is observed with the elevation of strain rate. At 0.8 mm/min, the average ultimate tensile strength (UTS) is 40.41 MPa. This value rises to 46.57 MPa at 2 mm/min, reaching its maximum UTS at 20 mm/min with 52.62 MPa. This consistent strengthening pattern implies that the PLA material demonstrates an enhanced ability to withstand tensile forces under higher strain rates. The dynamic behaviour observed suggests that the material becomes progressively more robust and resilient as the applied strain rate increases.

Based on Figure 7b, there is an increase in Elastic modulus as the strain rate increases. It increases from 1.54 GPa at 0.8 mm/min to 1.79 GPa at 2 mm/min, representing a rise of approximately 16.2%. The maximum value is observed at 2.21 GPa at 20 mm/min, indicating an increase of about 43.5% compared to the modulus at 0.8 mm/min. The observed incline in Elastic modulus with increasing strain rate suggests that the 3D printed PLA material's stiffness or resistance to deformation increases as the rate of applied force or strain increases. This implies that the mechanical behaviour of the PLA material is influenced by the rate at which stress is applied, with higher strain rates leading to a high stiff response.

Figure 8 presents data on the ultimate strain and testing time for PLA material at different strain rates (0.8 mm/min, 2 mm/min, and 20 mm/min). Based on Figure 8a the PLA

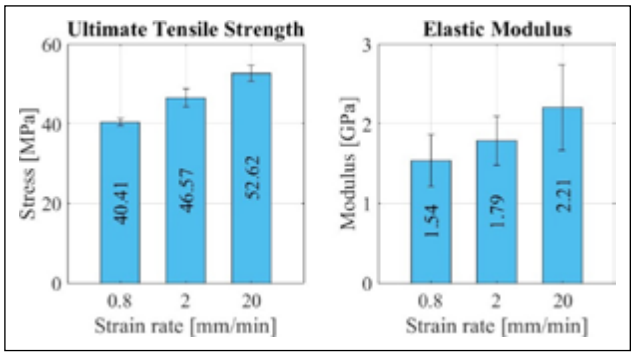

Figure 7. **(a)** Ultimate tensile strength and **(b)** Eastic modulus for each strain rate.

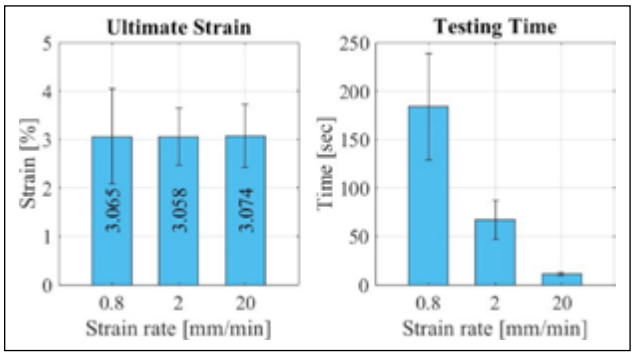

Figure 8. **(a)** Ultimate strain **(b)** Testing time and for each strain rate.

material exhibited behaviour that aligns with the findings of Hodzic et al. [5], which indicate that the impact of increasing strain rate on PLA varies. This is reflected in the experiment results, where the ultimate strain decreases from 3.065% at 0.8 mm/min to 3.058% at 2 mm/min, followed by an increase to 3.074% at 20 mm/min. However, these variations are minimal, demonstrating that the influence of higher strain rate on 3D-printed PLA material is negligible. A notable increase in standard deviation is observed, attributed to significant variation in strain values resulting from necking in certain specimens, while others experienced immediate fracture.

As anticipated, an increase in strain rate resulted in a reduction in the average testing duration, as shown in Figure 8a. Specifically, when the strain rate increased from 0.8 mm/min to 2 mm/min, the testing time for the PLA material decreased from 183.83 seconds to 66.67 seconds, reflecting a 64% reduction. Furthermore, at a strain rate of 20 mm/min, the testing time further decreased to 11.17 seconds, representing a significant 94% decrease compared to the initial rate of 0.8 mm/min. This trend aligns with expectations, as higher strain rates typically lead to faster and more dynamic material responses during testing.

The results of this study align with existing literature, showing that higher strain rates generally influence the mechanical properties of 3D-printed PLA materials. As strain rates increased from 0.8 mm/min to 20 mm/min, the ultimate tensile strength rose by 30%, consistent with findings by Ali et al. [4] and Hodžić et al. [5]. Moreover, Elastic modulus increased by 43.5% with higher strain rates, indicating greater stiffness. However, the ultimate strain before fracture showed negligible variation, suggesting that strain rate had little effect on the material's elongation. Additionally, higher strain rates significantly reduced testing time and resulted in more brittle material behavior, in line with studies by Vidakis et al. [6] and Ergene and Bolat [26]. Inconsistencies in data at higher strain rates may be attributed to challenges in accurately detecting speckle patterns during DIC analysis. These factors highlight the complexity of material behavior under varying strain rates. Overall, the study confirms that increasing strain rates enhance tensile strength and stiffness, while having minimal impact on ultimate strain, offering a deeper understanding of PLA's mechanical response under different testing conditions.

CONCLUSION

This study investigated the impact of strain rate on the mechanical properties of PLA material produced through FDM, employing strain rates of 0.8 mm/min, 2 mm/min, and 20 mm/min. DIC was used to assess tensile properties. The results revealed a consistent increase in Ultimate Tensile Strength (UTS) with higher strain rates, rising from 40.41 MPa at 0.8 mm/min to 52.62 MPa at 20 mm/min, showcasing the material's enhanced ability to withstand tensile forces. Concurrently, Elastic modulus exhibited a rising trend, increasing from 1.54 GPa at 0.8 mm/min to 2.21 GPa at 20 mm/min, reflecting an increase in stiffness with higher strain rates. On the other hand, Testing time decreased significantly with increased strain rates, dropping from 183.83 seconds at 0.8 mm/min to 11.17 seconds at 20 mm/min, a 94% reduction. The observed reduction in testing time at higher strain rates aligns with the dynamic nature of material responses during testing. Furthermore, ultimate strain values showed minimal changes, from 3.065% at 0.8 mm/min to 3.074% at 20 mm/min, indicating little to no influence of higher strain rates. These findings underscore the importance of considering strain rate sensitivity in the design and evaluation of 3D printed PLA, providing valuable insights for optimizing FDM processes and enhancing the material's mechanical performance under dynamic loading condition, offering valuable insights that can guide future research in this area.

Data Availability Statement

The authors confirm that the data that supports the findings of this study are available within the article. Raw data that support the finding of this study are available from the corresponding author, upon reasonable request.

Author's Contributions

Sara Saeed Abdulrahman Eltahir: Conception, Design, Materials, Data Collection and Processing, Analysis and Interpretation, Literature Review.

Roaa Gomaa: Conception, Design, Materials, Data Collection and Processing, Analysis and Interpretation, Literature Review.

Çağatay Yılmaz: Conception, Design, Supervision, Data Collection and Processing, Writer, Critical Review.

Conflict of Interest

The authors declared no potential conflicts of interest with respect to the research, authorship, and/or publication of this article.

Use of AI for Writing Assistance

AI not used for writing.

Ethics

There are no ethical issues with the publication of this manuscript.

REFERENCES

[1] Wong, K. K. V., & Hernandez, A. (2012). A review of additive manufacturing. *ISRN Mechanical Engineering*, 2012, Article 208760. [CrossRef]

[2] Singh, R., Singh, J., & Singh, S. (2016). Investigation for dimensional accuracy of AMC prepared by FDM assisted investment casting using nylon-6 waste based reinforced filament. *Measurement, 78*, 253–259. [CrossRef]

[3] Kristiawan, R., Imaduddin, F., Ariawan, D., Sabino, U., & Arifin, Z. (2021). A review on the fused deposition modeling (FDM) 3D printing: Filament processing, materials, and printing parameters. *Open Engineering, 11*, 639–649. [CrossRef]

[4] Ali, S., Abdallah, S., Devjani, D., John, J., Samad, W. A., & Pervaiz, S. (2022). Effect of build parameters and strain rate on mechanical properties of 3D printed PLA using DIC and desirability function analysis. *Rapid Prototyping Journal, 29*, 92–111. [CrossRef]

[5] Hodzic, D., Pandžić, A., Hajro, I., & Tasić, P. (2020). Strain rate influence on mechanical characteristics of FDM 3D printed materials (pp. 168–175). *Proceedings of the 31st International DAAAM Symposium 2020*. [CrossRef]

[6] Vidakis, N., Petousis, M., Velidakis, E., Liebscher, M., Mechtcherine, V., & Tzounis, L. (2020). On the strain rate sensitivity of fused filament fabrication (FFF) processed PLA, ABS, PETG, PA6, and PP thermoplastic polymers. *Polymers, 12*, Article 2924. [CrossRef]

[7] Ergene, B., & Bolat, Ç. (2022). An experimental investigation on the effect of test speed on the tensile properties of the PETG produced by additive manufacturing. *International Journal of 3D Printing Technologies and Digital Industry, 6*. [CrossRef]

[8] Wang, K., Xie, X., Wang, J., Zhao, A., Peng, Y., & Rao, Y. (2020). Effects of infill characteristics and strain rate on the deformation and failure properties of additively manufactured polyamide-based composite structures. *Results in Physics, 18*, Article 103346. [CrossRef]

[9] Wang, Y., Li, X., Chen, Y., & Zhang, C. (2021). Strain rate dependent mechanical properties of 3D printed polymer materials using the DLP technique. *Additive Manufacturing, 47*, Article 102368. [CrossRef]

[10] Hibbert, K., Warner, G., Brown, C., Ajide, O. O., Owolabi, G., & Azimi, A. (2019). The effects of build parameters and strain rate on the mechanical properties of FDM 3D-printed acrylonitrile butadiene styrene. *Open Journal of Organic Polymer Materials, 9*, 1–27. [CrossRef]

[11] Sagias, V., Giannakopoulos, K. I., & Stergiou, C. (2018). Mechanical properties of 3D printed polymer specimens. *Procedia Structural Integrity, 10*, 85–90. [CrossRef]

[12] Elmrabet, N., & Siegkas, P. (2020). Dimensional considerations on the mechanical properties of 3D printed polymer parts. *Polymer Testing, 90*, Article 106656. [CrossRef]

[13] Rohbeck, N., Ramachandramoorthy, R., Casari, D., Schürch, P., Edwards, T. E. J., Schilinsky, L., ... & Michler, J. (2020). Effect of high strain rates and temperature on the micromechanical properties of 3D-printed polymer structures made by two-photon lithography. *Materials & Design, 195*, Article 108977. [CrossRef]

[14] Vanaei, H., El Magri, A., Rastak, M., Vanaei, S., Vaudreuil, S., & Tcharkhtchi, A. (2022). Numerical–experimental analysis toward the strain rate sensitivity of 3D-printed nylon reinforced by short carbon fiber. *Materials, 15*, Article 8722. [CrossRef]

[15] Cai, R., Lin, H., Cheng, P., Zhang, Z., Wang, K., & Peng, Y., … & S. Ahzi. (2022). Investigation on dynamic strength of 3D-printed continuous ramie fiber reinforced biocomposites at various strain rates using machine learning methods. *Polymer Composites, 43*, pp. 5235–5249. [CrossRef]

[16] Lai, C. Q., Markandan, K., Luo, B., Lam, Y., Chung, W., & Chidambaram, A. (2020). Viscoelastic and high strain rate response of anisotropic graphene-polymer nanocomposites fabricated with 3D stereolithography printing. *Additive Manufacturing, 37*, Article 101721. [CrossRef]

[17] Baligidad, S., Gangadhara, C., & Chandrashekhar, M. (2021). Investigation on strain rate sensitivity of 3D printed sPEEK-HAP/rGO composites. *Research Square*. doi: 10.21203/rs.3.rs-1125996/v1 [CrossRef]

[18] Fisher, T., Almeida, H. Jr., Falzon, B. G., & Kazancı, Z. (2023). Tension and compression properties of 3D-printed composites: Print orientation and strain rate effects. *Polymers, 15*, Article 1708. [CrossRef]

[19] Hosseini, S. A., Torabizadeh, M., & Eisazadeh, H. (2023). Experimental study of the effect of strain rate on the mechanical behavior of assorted thermoplastic polymers. *Journal of Materials Engineering and Performance, 33*, 6942–6951. [CrossRef]

[20] Wang, K., Xie, G., Xiang, J., Li, T., Peng, Y., & Wang, J., et al. (2022). Materials selection of 3D printed polyamide-based composites at different strain rates: A case study of automobile front bumpers. *Journal of Manufacturing Processes, 84*, 1449–1462. [CrossRef]

[21] Patanwala, H., Hong, D., Vora, S., Bognet, B., & Ma, A. (2017). The microstructure and mechanical properties of 3D printed carbon nanotube-polylactic acid composites. *Polymer Composites, 39(Suppl 2)*,

E1060–E1071. [CrossRef]

[22] Mahmoudi, M., Burlison, S., Moreno, S., & Minary-Jolandan, M. (2021). Additive-free and support-free 3D printing of thermosetting polymers with isotropic mechanical properties. *ACS Applied Materials & Interfaces, 13*, 5529–5538. [CrossRef]

[23] ASTM International. (2014). ASTM D638-14 Standard test methods for tensile properties of plastic. *America Society for Testing and Material*. ASTM International.

[24] Yilmaz, C., Ali, H. Q., & Yildiz, M. (2022). Application of classical lamination theory to fused deposition method 3-D printed plastics and full field surface strain mapping. *Afyon Kocatepe Üniversitesi Fen ve Mühendislik Bilimleri Dergisi, 22*, 342–352. [CrossRef]

[25] eSUN. (Aug 21, 2024). PLA+, https://www.esun3d.com/pla-pro-product/

[26] Bolat, Ç., & Ergene, B. (2022). An investigation on dimensional accuracy of 3D printed PLA, PET-G and ABS samples with different layer heights. *Çukurova Üniversitesi Mühendislik Fakültesi Dergisi, 37*, 449–458. [CrossRef]